to aggregate during the laser pulse or soon afterwards, leading to the formation of larger clusters. In addition, heterogeneous decomposition, liquid phase ejection and fragmentation, homogeneous nucleation and decomposition, and photomechanical ejection are among the processes known to lead to nanoparticles production. Many of these processes would be governed by the intensity and pulse duration of the laser beam used for ablation. The lasers used for pulsed laser deposition for making solid clusters are normally of few fs to few ps duration. At Laser Plasma Laboratory, pulsed nanoparticle deposition of various metals has been carried out using sub-nanosecond duration pulses (300ps) at different focussing conditions.

The experiments were carried out using the uncompressed pulses (300 ps duration, 30 mJ energy) from a chirped-pulse amplification based 10TW Ti:sapphire laser system. The samples were placed inside a vacuum chamber and the laser pulses were focussed on the targets at two regimes of focussing. In the first case (referred to as tight focussing), the intensity of laser radiation was in the range of 2×10^{12} Wcm^{-2}, and in the second case (referred to as weak focussing), the intensity was considerably lower (4×10^{10} Wcm^{-2}). Silver, indium, stainless steel, and chromium were used as targets.

The structure of the deposited films was analyzed using different techniques. The absorption spectra of the deposited films were analyzed using a spectrograph. The analysis of the sizes of deposited nanoparticles was carried out using the total reflection x-ray fluorescence (TXRF). The structural properties of the deposited films were analyzed using a scanning electron microscope, a transmission electron microscope), and an atomic force microscope. The first three facilities are at SUMRD, RRCAT and the last one at LSED, RRCAT. Float glass, silicon wafer, and various metal strips (silver, copper, and aluminum) were used as the substrates for nanoparticle deposition for use with the above facilities.

The absorption spectra of the materials deposited on float glass were used to determine the presence or absence of nanoparticles from the appearance of strong absorption bands associated with surface plasmon resonance (SPR). In all metals, in the case of tight focusing, the peaks of SPR were centered in the range of 440 to 490 nm, indicating presence of nanoparticles. In the case of the deposition of silver film at the weak focussing conditions, no absorption peaks were observed in this region, indicating the absence of nanoparticles. The structure of the deposited films was analyzed using TXRF, which identified the presence of nanoparticle deposition in tight focussing condition of the laser. In the case of weak focussing, it showed a thin film-like deposition of metal, without any presence of nanoparticles. X-ray fluorescence measurements and SEM studies gave the average size of the silver nanoparticles to be 60 nm. The TEM measurements also confirmed the presence of silver nanoparticles in these deposited films. The atomic force microscopy also gave the average size of silver nanoparticles to be 65 nm. The details of this study can be found in *Applied Optics 46, 1205, 2007.*

Indium nanoparticles are quite important as they have a number of practical applications like potential nano-lubricants, as possible candidate for single electron transistors, as tags for detection of DNA hybridization, as printing blocks in nano-xerography, and as starting material for convenient synthesis of InP. Hence, a detailed study of the structural, optical and nonlinear optical properties the indium nanoparticles prepared by the laser ablation of bulk indium target in the vacuum at the tight focusing conditions and those prepared by laser ablation in liquids, was carried out. Details of this study are given in *Applied Phys. B 86, 337, 2007*

Contributed by:
U.Chakravarty (uday@cat.ernet.in) and P.A.Naik

L.5. : Use of a hollow conic beam to enhance atom transfer in BEC set-up

To achieve Bose-Einstein condensation (BEC) of Rb^{87} atoms, a double magneto-optical trap (MOT) system has been made operational recently at Laser Physics Applications Division. In this set-up (Fig.L.5.1), a vapour-cell MOT is loaded in a chamber (at pressure 2×10^{-8} torr) where Rb vapour is generated using a getter source. The trapped and cooled atoms in this MOT are then subjected to a continuous wave resonant push beam to load another MOT in a UHV chamber (~8×10^{-10} torr) where RF evaporation will be used for further cooling. The number of atoms in this MOT and in the vapour-cell MOT were measured by

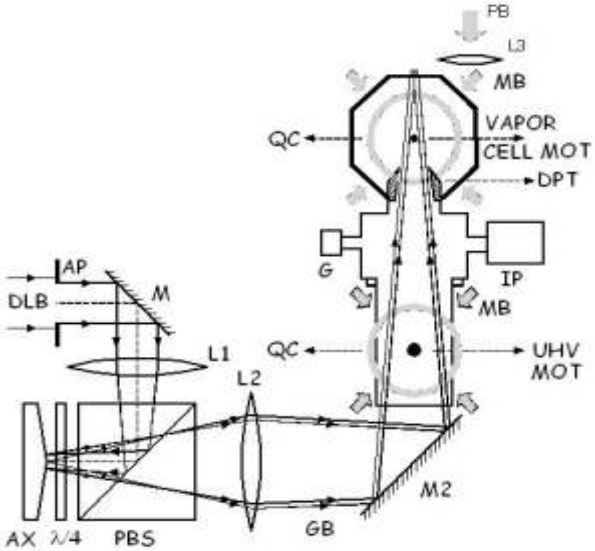

Fig.L.5.1. Schematic of the set-up to guide cold atoms from vapour cell MOT to UHV MOT. DLB: diode laser beam, AP: aperture, M & M_2: 45° high reflectivity mirrors, AX: axicon mirror, λ/4: quarter wave plate, PBS: polarizing beam splitter, L_1: lens of 80 mm focal length, L_2: lens of 250 mm focal length & 75 mm diameter, L_3: lens of 300 mm focal length & 50 mm diameter, GB: guiding hollow beam, MB: MOT beams, PB: push beam, IP:sputter ion pump, G: gauge, QC: quadrupole coils, DPT: differential pumping tube.

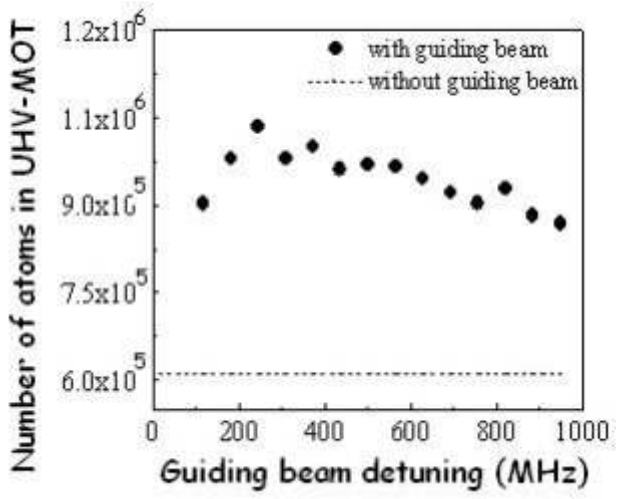

Fig. L.5.2. Variation of number of atoms in UHV-MOT with detuning of the guiding hollow beam from the cooling transition of Rb^{87}.

fluorescence imaging with a CCD camera. Loading of the UHV-MOT was found to depend on power of the push beam and the optimum power was found to be ~ 160 μW.

To enhance the number of atoms in UHV-MOT further, a blue-detuned hollow guiding beam was used to confine atoms in transverse direction while they are being transferred from vapor-cell MOT to UHV-MOT. This hollow guiding beam was generated using a metal axicon mirror *(Ref. RRCAT Newsletter Issue 2, 2006, p.5)* and focused using a lens combination. The hollow guiding beam (power ~ 33 mW) was blue-detuned from the cooling transition of Rb^{87} and the number of atoms in UHV-MOT was measured for different values of detuning of the guiding beam. As shown in the Fig.L.5.2, for a suitable detuning, around two-fold enhancement in the atom number was observed.

Contributed by:
S.R.Mishra (srm@cat.ernet.in)

L.6: In-vivo, non-invasive measurement of gradient refractive index profile of crystalline lens of fisheye

Crystalline lens of an eye plays an important role in visualization. The crystalline lens does the primary focusing for aquatic animals, as immersion renders cornea optically ineffective. The commonly employed techniques for measurement of gradient index profile are Abbe refractometer, interference technique, and laser ray tracing methods that require either sectioning or dissection of the lens. Magnetic resonance imaging (MRI) can be used for the non-invasive measurement of refractive index profile of fisheye lens. However, conventional MRI is not suitable for measuring the refractive index in the core region of the lens due to the absence of free water.

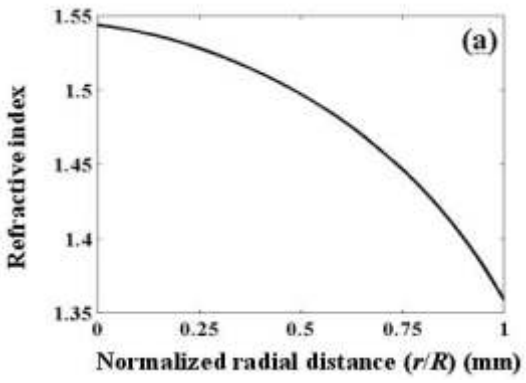

Fig.L.6.1: Refractive index profile obtained from the fitted mean values of coefficients using a polynomial refractive index model (R is radius of the lens).